The International Journal of Advanced Manufacturing Technology
https://doi.org/10.1007/s00170-025-15089-7

ORIGINAL ARTICLE

Hybridizing 3D printing and electroplating for the controlled forming of metal structures within fused deposition modelled contours

Tobias Müller[1] · Steffen Scholz[1] · Marco Ehrhardt[2] · Sonia Ruíz Trujillo[3,4] · Mar Cogollo de Cádiz[5] · Andrés Díaz Lantada[3] · Markus Guttmann[2]

Received: 18 October 2024 / Accepted: 18 January 2025

Abstract
An innovative approach for metal electroforming is presented, exemplified with proof-of-concept geometries and illustrated with an industrial application. The proposed production chain hybridizes 3D polymer printing and nickel electroplating for the design-controlled forming of metals within fused deposition modelled contours or patterns, which provide a selective functionalization of the substrate for metal deposition on demand. Applying the developed process, Ni electrodes for streamer discharge plasma generators are structured. These components stand out for their needle-like details, required for promoting streamer discharge phenomena, which would be challenging to obtain employing traditional milling processes. Current capabilities, main challenges and foreseen research directions, for this novel hybrid 3D printing and electroplating process and for its industrial applications, are discussed. Overall, the described process contributes to the already fruitful connections among additive manufacturing technologies and metal electrodeposition procedures, providing an interesting route towards accessible and straightforward electroforming of large components and structures.

Keywords Electroplating · Electroforming · 3D printing · Streamer discharge

1 Introduction

Electrodeposition of metals from solution is a well-established family of industrial methods that has been rendering innovations to the ways metals are purified, structured, processed, protected, functionalized, and recovered for more than one century and with continuous progresses. In their classical work on "Principles of electroplating and electroforming (electrotyping)", Blum and Hogaboom divided electrodeposition in four main fields: electrorefining, electrowinning, electroplating and electroforming, the latter introduced then as "new concept" for the production or reproduction of components by electrodeposition [1, 2]. According to Mc Geough's definition: "In electroforming, metal is deposited electrolytically upon the cathode-polarized electrode of an electrochemical cell. Unlike electroplating, in which the deposited metal has to adhere to the cathode after electrolysis, in electroforming much thicker coatings are applied, the plating is performed on a cathode, and the surface of which bears a non-conducting film so that the deposited metal can be subsequently removed to yield a free-standing artifact or structural component", and its discovery is dated back to 1838 by Jacobi [3]. Several variations of the electroforming process and a wide set of metals processable through electroforming foster industrial applications in energy, transport, space and healthcare, to cite a few areas.

Along the last decades, both electroplating and electroforming have synergically evolved with the methods and technologies from the micro and nano-electro-mechanical-systems (MEMS/NEMS) industry, enabling many relevant

✉ Andrés Díaz Lantada
andres.diaz@upm.es

✉ Markus Guttmann
markus.guttmann@kit.edu

1 Institute for Automation and Applied Informatics, Karlsruhe Institute of Technology, Karlsruhe, Germany

2 Institute of Microstructure Technology, Karlsruhe Institute of Technology, Karlsruhe, Germany

3 Department of Mechanical Engineering, Universidad Politécnica de Madrid, Madrid, Spain

4 Research & Development Department, Cedrión Consultoría Técnica E Ingeniería S.L., Madrid, Spain

5 Educational Department, Tecnatom, Tarragona, Spain

Published online: 28 January 2025

advances these areas, as these MEMS and NEMS usually require thin metal coatings, selective metallic functionalization or even metallic structures [4, 5]. Indeed, electroplating and electroforming as excellent companions to other usual technologies from the MEMS/NEMS realm like etching, photolithography, chemical and physical vapor deposition or surface or bulk micromachining.

In fact, the use of electroforming is especially well-suited for the creation of ultra-fine inserts and molds for mass production. Such molds or inserts are normally grown upon (or within) lithographically obtained masters in softer materials or directly upon the surfaces of natural or synthetic objects. This rationale has been pivotal for the developing of different production chains, from micro-manufactured master models to mass production tools, including LIGA (from German *Lithographie*, *Galvanoformung, Abformung*) and deep X-ray LIGA [6–8], compression molding or hot embossing [9, 10], polymeric and ceramic micro-injection molding [11, 12], and different biotemplating processes [13–15], to mention some relevant possibilities.

Recently, synergies between electroforming and high-precision additive manufacturing technologies, including combinations of UV-lithography, laser stereolithography and two-photon polymerization, have been also employed by our team for achieving multi-scale devices [16, 17] and functional biointerfaces [18, 19]. Applications in the development of lab-on-a-chip and organ-on-a-chip devices, cell culture platforms and microtextured biomedical devices have been explored and demonstrated.

Such fruitful connection among additive manufacturing technologies and metal electrodeposition procedures is currently a very popular research topic, with growing ramifications leading to versatile production processes. For example, additive electrochemical micro-manufacturing is emerging for the precise growth of pure metallic components [20] and multi-metallic structures [21], the electrochemical reconfiguration of architected materials has been demonstrated [22], and extrusion-based 3D printing has been hybridized with electroplating for metalizing the polymeric filament layers and reaching design-controlled metallic structures [23].

However, the research impact and industrial uptake of some of these innovative production chains are sometimes neglected by the limited availability of the first technological stage (master generation), often due to their extreme installation and operation costs, as in the case of LIGA, two-photon polymerization and industrial laser stereolithography. In other cases, the reachable part sizes are also very limited, considering that some UV photopatterning systems and 3D direct laser writing systems achieve outstanding detail but are restricted to structuring a few mm^3.

To progress towards the desired accessibility, ease of use and electroforming of larger components and structures, this study presents for the first time an innovative production chain hybridizing 3D printing and electroplating for the controlled forming of metals within fused deposition modelled contours. In this approach, the selective patterns generated by extruding thermoplastic filaments upon the substrates for metallization are found able to guide the metallization process for reaching design-controlled structures. Good practices for fused deposition modelling, electroforming and postprocessing are provided to minimize production failures and render the research as repeatable as possible, which is expected to synergize with the accessibility of the employed resources for increased impacts.

The presented procedure may complement other additive manufacturing approaches aimed at the creation of complex-shaped metallic components, including the laser powder bed fusion of nickel super-alloys [24], the additive manufacturing of 3D nanoarchitected metals employing lithographic procedures of Ni-rich photoresits followed by pyrolysis [25], or the use of wire and arc additive manufacturing and robotic manipulation, also applicable to Ni and other alloys [26, 27].

Apart from explaining the method and exemplifying it with various proof-of-concept geometries, the industrial applicability is analyzed through the development of a set of reliable Ni electrodes for streamer discharge plasma generators [28, 29]. These structural electrodes may constitute an attractive alternative to the thin metallic filaments employed in atmospheric plasma corona discharge devices [30, 31]. In these devices, the filaments acting as corona electrodes are often the weakest component and lack structural function [32], while the Ni-structured electrodes presented here prove mechanically stable. The systematic characterization of the obtained electrodes validates both the functionality of the components achieved and the proposed production route, which provides a feasible way of structuring Ni with fine details that would be challenging to obtain by computed-numerical control machining or milling processes [33, 34].

Finally, the main limitations of the study, the most urgent current research challenges and some impactful future proposals for further investigation are discussed. Before presenting the key findings and discussing them, the employed materials and methods are detailed in the following section.

2 Materials and methods

2.1 Method for 3D printing–assisted electroplating

The proposed 3D printing–assisted electroplating synergizes different materials and technologies for the design-controlled electrochemical deposition (or growth) of metals within the boundaries or contours of physical masks obtained by fused deposition modelling of thermoplastic filament upon plates of wafers. The process involves the following operations: (1) design of the physical mask with the support of a 2D

or 3D drawing or computer-aided design (CAD) modelling software or a mask generation program. (2) 3D printing of the designed physical masks upon wafers, plates or metallic substrates, normally employing fused deposition modelling due to its wide availability and affordability, although other additive manufacturing technologies may apply. The generated physical masks create protected and unprotected regions upon the metallic substrates and define the boundaries for the subsequent stage. (3) Electrochemical deposition of the desired metal, in this study nickel. (4) Rinsing, wafer etching and elimination of thermoplastic material to reach the desired grown metallic components.

The experimental details of the different stages employed for this study are provided below, including specific design decisions, determinant parameters and operating conditions of the setups required for manufacturing the proof-of-concept geometries and for creating the samples for the selected industrial application, linked to innovative and robust electrodes for streamer discharge and plasma generation.

2.1.1 Design of physical masks

Computer-aided designs of the physical masks, to be printed upon metallic substrates for subsequent electroplating, were obtained with the support of NX (Siemens PLM) modelling software. First, different versions of masks for obtaining spiky electrodes for streamer corona discharge were designed. Second, representative examples were integrated into a single mask design for enabling production of several electrodes with variations in a single printing and electroplating step. These electrodes counted with an L-shape structure and two spikes normal to the longer arm of the L, from which the streamer discharge would be promoted. Design variations included sharper spikes with a base of c.a. 1 mm, medium spikes with a base of c.a. 2 mm and broader spikes with a base of c.a. 3 mm, to analyze the influence of aspect ratio on ignition voltage. Each mask was designed to incorporate 9 electrodes with 3 replicas of each design. Conversion to.stl files enabled subsequent 3D printing as described below.

2.1.2 3D printing upon metallic substrates

3D printing of polymeric masks was carried out on 4″ silicon wafers coated with a Ti/TiO_x layer. For keeping costs low and to test the capabilities of this method, Fused Filament Fabrication (FFF) was chosen as the method for the additive manufacturing step. Prints were carried out on a Prusa i3Mk3S (Fig. 1) printer equipped with a 0.25-mm nozzle to increase the resolution in X/Y direction to adjust for the finer details of the mask. In addition, a specialized wafer holder was machined and placed on the print bed, securing the wafer at a distinct position, as movement of the wafer would have caused shifting between the individual layers printed. Slicing of the original CAD model (delivered as an.stl file) was performed with the respective Prusa Slicer. The most relevant parameters set for the printing step of the final test structures are shown in Table 1. The parameters were chosen after conducting a series of preliminary tests involving various polymer

Table 1 Parameters for printing step of the final test structures

Parameter	Printhead temperature [°C]	Bed temperature [°C]	Layer Height [µm]	Print Speed [mm/s]	Extrusion multiplier [%]
Setting	235	90	100	20	100

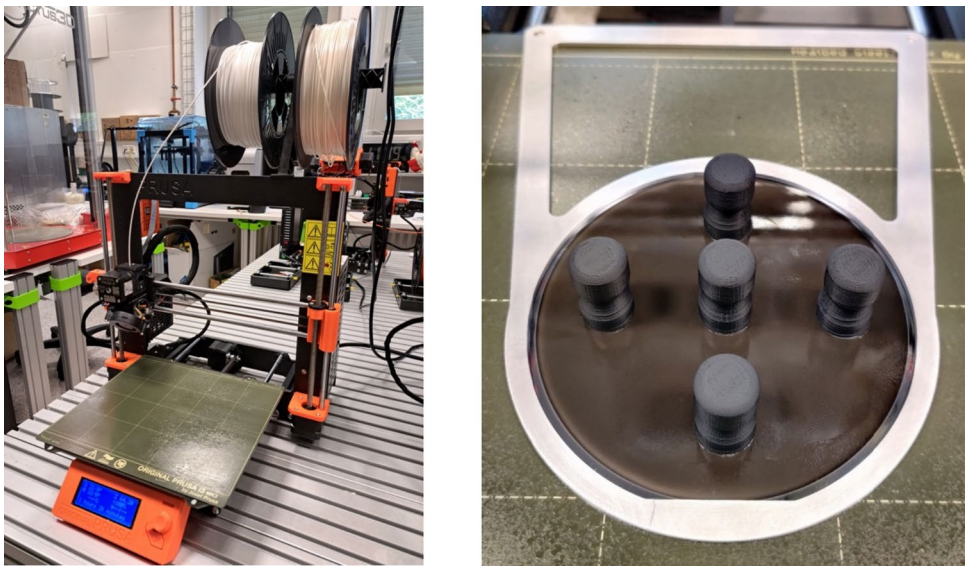

Fig. 1 3D printing setup: Prusa i3 MK3s FF printer (left) and machined wafer holder for 4″ silicon wafers (right)

types as well as an optimization of the printing parameters for ASA.

After the slicer generated the G-code for the printing step, modifications to the code were necessary to adjust for the wafer holder, meaning that the print sequence was modified like follows, and employing the materials described further on: (1) Initial bed distance measuring routine using the Prusa auto-leveling sensor. (2) Movement of printhead to elevated z-position for placing the wafer holder. (3) Attaching and securing the wafer holder. (4) Material extrusion on front part of platform to secure material flow. (5) Elevating the printhead slightly above the height of the wafer holder. (6) Moving printhead to start position on the wafer. (7) Lowering printhead to z-position calculated by initial bed distance plus wafer thickness. (8) Start of print.

Initial tests were carried out with different filament materials commonly used in FFF, according to details given in Table 2. In particular, poly(methyl methacrylate) (PMMA), acrylonitrile butadiene styrene (ABS), acrylonitrile styrene acrylate (ASA) and polycarbonate (PC) were tested on the silicon wafer with different coatings (used as adhesion layers). Each of these polymers is widely used polymers in the 3D printing community while also being dissolvable by solvents typically available in a chemical laboratory. Therefore, these materials were chosen over other potential candidates that are known for their difficult printing behavior or chemical resistance. The testing was carried out to clarify two main questions, namely the adhesion on the wafers themselves and, secondly, the solubility of printed parts in common solvents, as the printed masks have to be dissolved after the electroplating step.

Adhesion tests were carried out according to DIN 50002–2 to determine the most suitable polymer for printing the masks. To test the materials, small (4 mm × 4 mm × 3 mm) cubes (Fig. 2a) were printed on the wafer and adhesion was tested by shearing off the cubes with a testing machine (TA.XT.Plus form stable micro systems) according to the DIN (Fig. 2b).

2.1.3 Electrochemical deposition

Once the masks were printed, electrochemical deposition followed, employing methods based on previous joint experiments [16, 17], with some important modifications. To foster electroplating, base samples consist of standard 4″ silicon wafers (~ 500-µm thick), whose top side is coated with a titanium layer (1-µm thick). The titanium is then wet-chemically oxidized, creating a conductive Ti/TiOx layer, upon which FFF is performed.

After 3D printing, the adhesive applied on top of the entire surface, in order to make the 3D-printed material better stick to the Ti/TiOx layer, needs to be removed before electroplating. To this end, an oxygen plasma etching process at 100 W and 100 mTorr for 1 h is employed, to achieve the desired conductive surface for the electroplating process in between the printed material. A Sentech Etchlab 200 machine was employed for this purpose. The adhesive underneath the 3D-printed material is left untouched to not interfere with the adhesion thereof whereas the material elsewhere is etched away.

When the required conductivity is confirmed, the sample is then fixed inside of an electroplating holder, which is submerged in the electrolyte bath in order to start the electroplating process. Knowing the surface area minus the area of the 3D-printed material, desired height for the electroplated nickel is accurately calculated. The 3D-printed material always has to be printed as a negative of the desired structures (corona streamer electrodes in this study), as the nickel grows within the 3D-printed boundaries, and not on top of it to avoid overplating, due to the lack of conductivity.

The used nickel electrolyte is a self-made boric acid containing nickel sulfamate electrolyte (well-known for electroforming) with ~ 80 g/l nickel, ~ 40 g/l boric acid and 0.2 g/l

Table 2 An overview of the materials used, typical properties as stated by the filament manufacturers and the individual manufacturers

Polymer properties of tested materials					
	Unit	ABS	ASA	PMMA	PC
Printing temperature	°C	230	240	230	260
Glass transition temperature	°C	97	94	77	113
Tensile strength	MPa	43.6	40	35	59.7
Solvent		Concentrated acids, Esther Acids and aromatic and chlorinated hydrocarbons	Polar solvents, strong acids and bases, polar solvents, aromatic and chlorinated hydrocarbons	Strong acids and bases, polar solvents, Esther, Ether, aromatic and chlorinated hydrocarbons	Chlorinated hydrocarbon, strong acids and bases, different solvents
Shrinkage	%	0.4 to 0.7	0.4 to 0.8	0.1 to 0.8	0.6 to 0.8
Supplier		3DJake	Filamentum	Material4Print	Polymaker

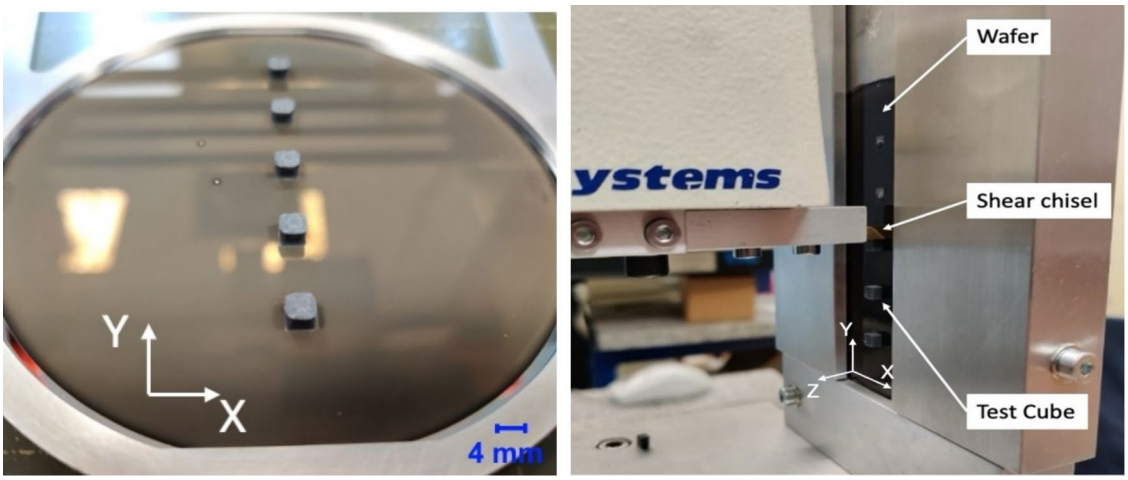

a) b)

Fig. 2 **a** Setup for adhesion tests: top-down view of test cubes (DIN 50002–2) on wafer. **b** Adhesion test setup. Coordinate system of printer indicated via X/Y/Z axis

surfactant. The pH is around 3.5, temperature c.a. 52 °C and the current density from 0.1 to 2.0 A/dm^2.

The heights of the 3D-printed material used throughout this study vary from 500 µm to around 2 mm, and the close to 2-mm-thick electrodes are finally employed for the corona discharge experiments. Due to uneven nickel distribution (please see discussion on limitations in Sec. 4.1), the theoretical height of the electroplated nickel layer should range from around 200 µm to no less than 100 µm smaller than the height of the 3D-printed material, e.g. corresponding to a thickness between 1.8 and 1.9 mm for a 2-mm sample.

During the electroplating process, different current densities are used to speed up the nickel growth, usually starting with lower values such as 0.1 A per square decimeter (A/dm^2) in order to allow the nickel layer to start growing properly at the base, all the way up to 2.0 A/dm^2 whenever a certain height has been reached in order to save time. This translates to nickel deposition rates between roughly 1.23 and 24.58 µm per hour.

After electroplating, the sample is rinsed with DI water and isopropyl alcohol. It is then submerged in ethyl acetate inside of a ~ 60 °C ultrasonic bath in order to remove the 3D-printed material: ASA (acrylonitrile styrene acrylate) after evaluation of different candidates. The time of this step ranges, according to the respective height of the ASA, from 4 up to 12 h. The nickel is not affected by this process and whenever the 3D-printed material is fully removed, the sample is once again rinsed with DI water and isopropyl alcohol.

Once the ASA has been removed, the sample is then submerged in a 30% potassium hydroxide solution at ~ 80 °C in order to remove the wafer substrate. Like before, this step can take varying amounts of time although it typically lasted for 6 h. Once again, the electroplated nickel is not affected, and the individual nickel structures are all that is left by the end of this process.

Finally, these structures are cleaned with isopropyl alcohol.

2.2 Testing of electroplated streamer discharge electrodes

Three types of L-shaped electrodes, each counting with two streaming discharge generation tips, differentiated by the sharpness of the discharge tips, were tested to analyze the ignition voltage for starting the streamer discharge and related plasma generation. Three replicas of each electrode were tested employing a 3D-printed setup (holder) for systematically changing the gap between the tips of the corona electrodes and the collecting electrode consisting of a planar Cu layer upon the base of the 3D-printed holder.

A high-voltage power supply (Heinzinger® LNC high voltage laboratory 6000–10 pos model) is used to produce the positive DC discharge. The manufactured L-shaped electrodes with the punctual tips (emitter or corona electrode) are connected to the high-voltage DC system, which operates at a voltage between 0 and 6 kV and the convergent or collecting electrode (planar Cu layer) is grounded. Two types of experiments are performed with the voltage power supply working with limited voltage or with limited intensity. In short, at each experimental run, voltage is progressively increased until the electric arc is generated, and the discharge stabilized, to obtain the ignition voltage for each type of electrode and as a function of the gap. Three ignitions for each sample and testing condition are documented.

Standard deviations are below 5% for the experiments performed with limited voltage and below 15% for the experiments performed with limited intensity.

3 Results and discussion

3.1 Results of the hybrid 3D printing and electroplating process

Firstly, the described methods and materials are applied to the manufacturing of proof-of-concept test structures for illustrating the variety of geometries achievable through the proposed hybridization between 3D printing and electrochemical deposition. A fundamental aspect for success is the adhesion between the printed layers and the wafers employed as substrate, for which the adhesion tests were performed. Remarkably, the adhesion test of printed samples showed that the connection withstands a shear force between 6.57 MPa in the case of ABS and 1.18 MPa in the case of PMMA. ASA and PC could withstand 4.3 MPa and 4.24 MPa, respectively (see Fig. 3).

A good adhesion is critical for avoiding underflow during the electroplating step, so ABS and ASA seem to be the preferable materials considering the connection between the printing material and the wafer surface. As the material also has to be removed after the electroplating step, printed samples were also treated with different solvents. Here, ASA exhibited a preferable behavior being easily dissolved in dichloromethane. Furthermore, when selecting the (thermoplastic) polymer 3D printing material, the stability of the polymer in the electrolyte has a direct influence on the subsequent electroplating process. The polymer (i.e. the printed structures) must not deform at the working temperature of the electrolyte (52 °C in this case) and there must be no chemical attack (no chemical reaction with the electrolyte components). In addition, no components should be released from the printed material that could then enter the electrolyte, contaminate it and thus influence the properties of the Ni deposit. For subsequent process steps and the separation of the metallic components, it is necessary that the printed plastic material can be dissolved in a common solvent after electroforming. In order to achieve good adhesion of the printed structures to the conductive substrate, an adhesion promoter is usually used regardless of the 3D printing material. This is sprayed or spun onto the substrate as a thin layer over the entire surface in advance. This thin layer must then be completely removed again inside the cavities in order to expose the conductive surface again.

Printing of masks was carried out on the setup described in Sec. 2.1. Due to the shrinkage of the polymer material, the silicon wafers were bending if a whole mask was printed as a full area on the wafer. Therefore, several iterations were tested, as shown in Fig. 4. By dividing the overall print area and introducing stress relief lines, a warping of the wafer, and therefore the final electrode, could be prevented.

Besides, as shown in Fig. 5, the process stands out for the selective electroplating thanks to the protective 3D-printed structures upon the conductive wafers. Metallic samples with desired geometries including file details are achievable and the employment of 3D printing for defining the boundaries stands out for being straightforward to apply, due to direct transfer from the original CAD model to the printed structure, and for its accessibility taking into consideration the widespread use of FFF and its overall low cost.

In agreement with the methods section, the deposition area is defined by the open area on the plating holder for the 4-inch substrates minus the area covered by the

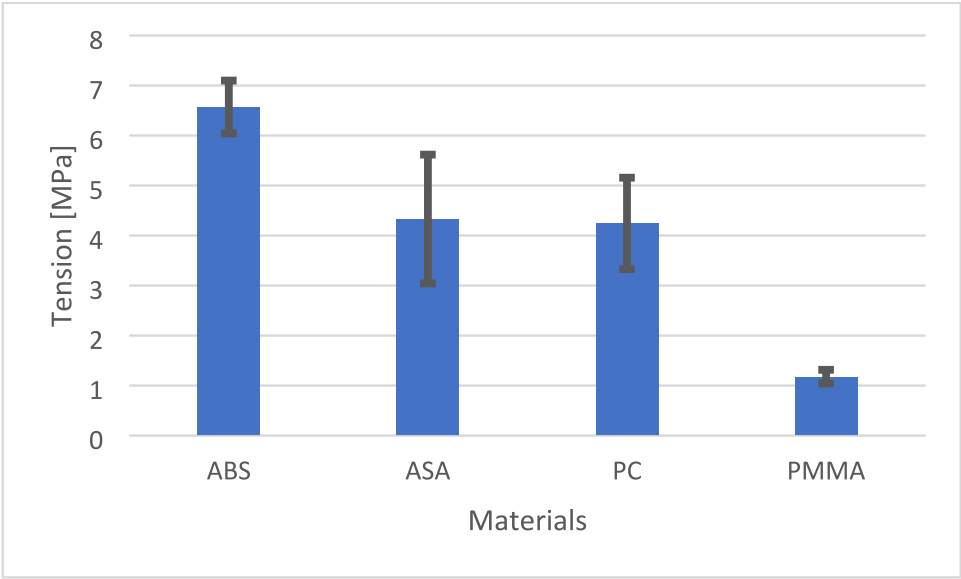

Fig. 3 Average shear stress in adhesion test for printed specimen

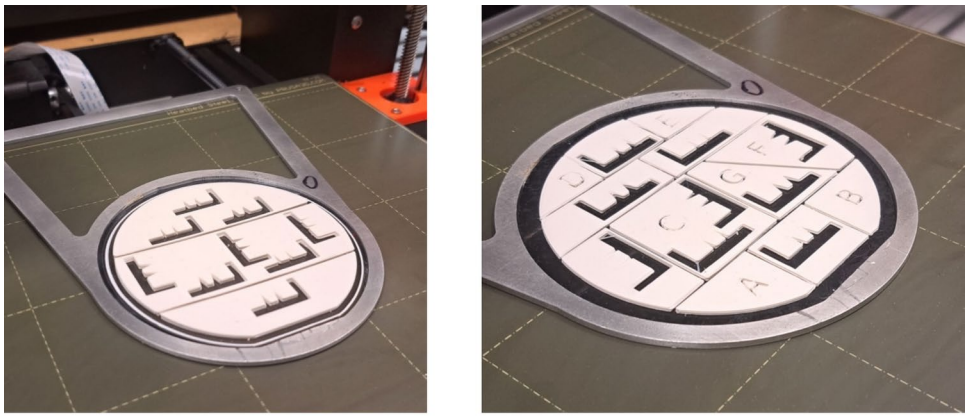

a) b)

Fig. 4 Iterations of electrode mask: second version with three individual parts (**a**), final version with smaller areas (**b**)

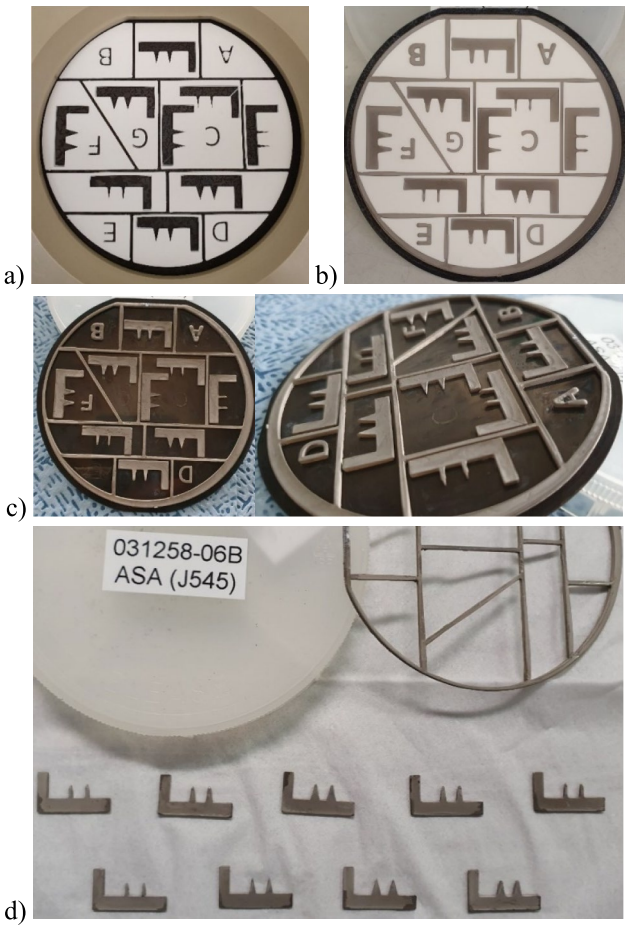

Fig. 5 Electroplating process and results: **a** substrates with printed masks, **b** electroplated wafers, **c** wafers with nickel structures after removal of 3D-printed material, and **d** achieved metallic samples of desired L-shape electrodes with streamer tips ready for the experiments described in Sec. 3.2

3D-printed material. In our case, this resulted in an area to be electroplated of approx. 2720 mm^2. The current density is precisely specified for a fixed time by setting a defined current at the voltage source. In these experiments, our team usually started at 0.1 A/dm^2 and then increase to 0.25 A/dm^2 after 1 h and then up to 2.0 A/dm^2 after further periods of time. Taking Faraday's laws into account, a deposition time can then be calculated for a defined deposition area in order to achieve a specific deposition height. Low current densities (< 2.5 $A/dm^2 = \max$ 30 µm/h) are recommended in order to achieve uniform growth of the nickel layer and thus uniform filling of the structure cavities. Furthermore, the electroplating holder should be moved horizontally during deposition and the electrolyte should be continuously circulated. Already in the layout for 3D printing, care must be taken to ensure that the cavities are evenly distributed on the substrate in terms of shape and size and, as general recommendation, the aspect ratio should not be greater than 3. A suitable wetting agent should be added to the nickel electrolyte to ensure good wetting and good penetration of the electrolyte into the cavities and to prevent gas bubbles from forming in the cavities.

Taking into account the quality of the electroplating process, scanning electron microscopy (SEM) is employed upon manufactured Ni electrodes as control measurement. Figure 6 presents a selection of SEM images performed upon the obtained Ni components. Figure 6a and b focus on different corners of the obtained electrodes at various magnification values (different rows), showing a conformal electroplating with homogeneous surface and minor defects. The way in which electroplating mimics the original 3D-printed template can be appreciated in the vertical Ni walls due to the presence of the wavy surface corresponding to the 3D-printed layers etched after the electroplating process.

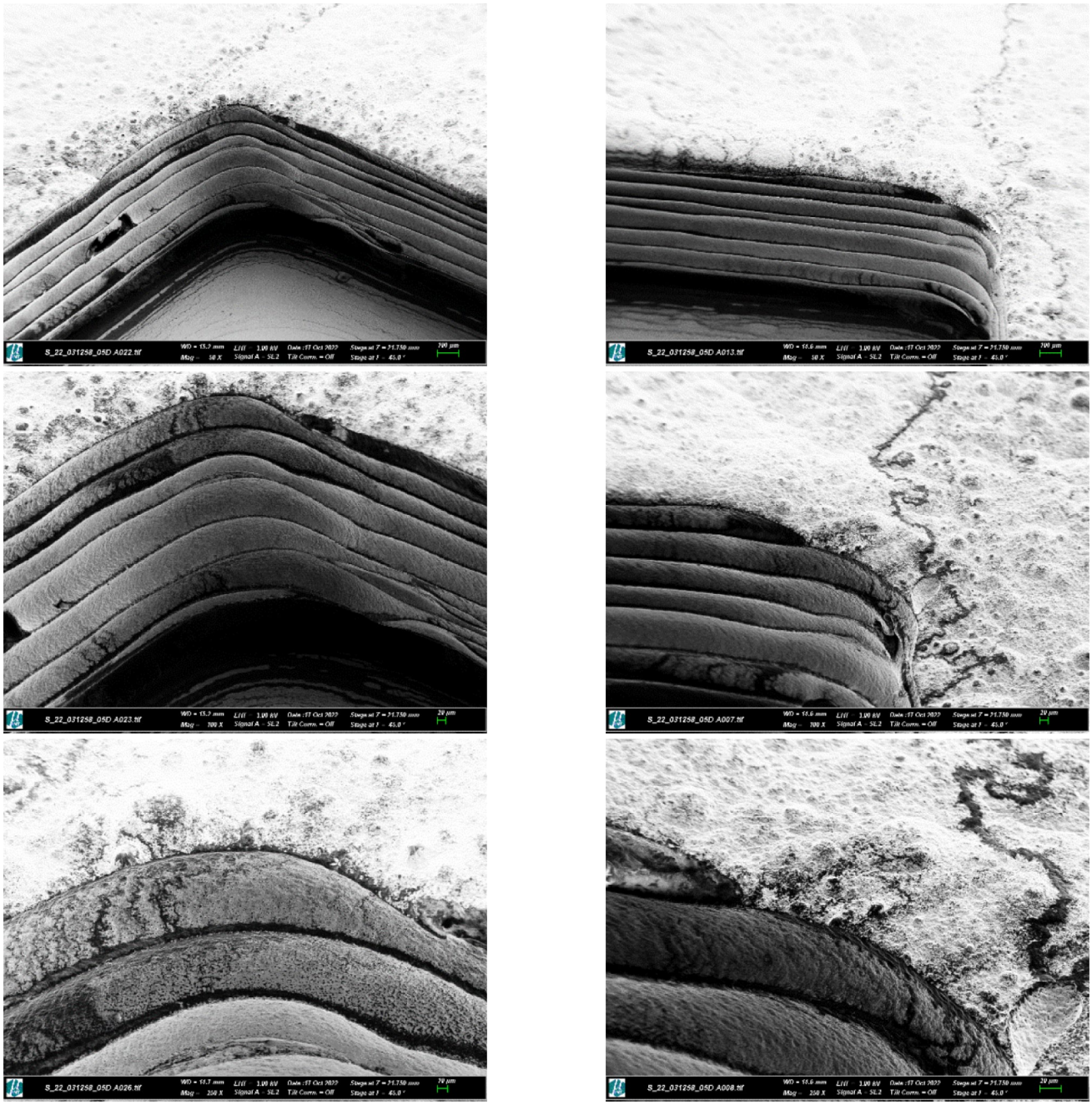

Fig. 6 Selection of SEM images performed upon the obtained Ni components. **a** and **b** Different corners of the obtained electrodes at various magnification values, showing a conformal electroplating with homogeneous surface and minor flaws further explained in Sec. 4.1. The way in which electroplating mimics the original 3D-printed template can be appreciated in the vertical Ni walls due to the presence of the wavy surface corresponding to the 3D-printed layers etched after the electroplating process

Minor issues and manufacturing flaws that may eventually occur are additionally discussed in Sec. 4.1, when dealing with the limitations of the presented study and current research challenges.

3.2 Results of the streamer discharge electrodes obtained by 3D printing–assisted electroplating

Secondly, the 3D printing–assisted electroplating is applied to the growth of special multi-tip electrodes conceived for promoting streamer discharge in plasma generators, selected as a possible industrial application for the proposed hybridization between fused deposition modelling and electrochemical deposition of metals.

As illustrated in Fig. 5d, the designed electrodes are achieved with a remarkable degree of precision. Considering the performance of the created electrodes, Table 3 summarizes the streamer corona discharge experiments performed with the values that lead to the experimental graphs included in Fig. 7. Three different tips, from sharper to broader, and five different gaps were evaluated in the two operating regimes of the power source described (limited voltage and limited intensity), as described in the experimental section. As can be seen in Fig. 7c, as expected, larger gaps lead to increased ignition voltages and the values obtained for the limited voltage operation are, in general, higher than those required for arc generation in the limited intensity mode (Fig. 7d). As regards tip type, the influence is not that clear. Apparently, the intermediate size tips require slightly lower ignition voltages at lower gaps, and a bit higher at larger gaps. The fact is that thinner tips are mechanically less robust and degrade more easily, which affect long-lasting performance and stability of the discharge, so with the obtained data the broader tips would be preferable.

Table 3 Summary of the streamer corona discharge experiments performed with the values that lead to the experimental graphs included in Fig. 7

Gap [mm]	Ignition voltage [kV] for 1-mm-thin electrode	
	Lim. voltage	Lim. intensity
0.5	2.97	2.58
1.0	3.30	3.19
1.5	3.91	3.90
2.0	4.20	4.22
2.5	4.42	4.41
Gap [mm]	Ignition voltage [kV] for 2-mm-thin electrode	
	Lim. Voltage	Lim. Intensity
0.5	2.94	2.62
1.0	3.52	3.27
1.5	4.08	3.97
2.0	4.68	4.56
2.5	4.73	4.71
Gap [mm]	Ignition voltage [kV] for 3-mm-thin electrode	
	Lim. Voltage	Lim. Intensity
0.5	3.20	2.93
1.0	3.33	3.24
1.5	4.32	4.37
2.0	4.56	4.50
2.5	4.69	4.61

After the experiments, visual inspection leads to finding small colored regions of c.a. 1 mm^2 upon the Cu plates employed as collecting electrodes, mainly surrounding the points of incidence of the generated electric arcs. This denotes, to some extent like in previous studies [28], mechanical and thermal damage, as well as material transfer from the tips to the plates, which inspires us to further explore the possibility of applying these kinds of streaming discharges for selective surface functionalization. Related procedures like spark plasma discharge and spark plasma sintering have already put forward the interest of controlled streamer discharge generation.

Related to previous studies by our team, in connection with plasma generation by corona discharge [26, 27], the structural L-shape electrodes with multiple tips lead to quite analogous ignition voltages for similar gaps, which puts forward the possibility of substituting the more common corona discharge wires by other morphologies and structures of emitter electrodes, the fine tips in current study.

It is important to highlight that these electroplated structural L-shaped electrodes prove more robust than the previously employed W filaments, which are prone to failure due to filament degradation or increased mechanical tension through heating and device dilatation. For some applications, in which punctual electric arc and consequent plasma generation may be required, the electrodes grown by electroplating within the boundaries of 3D-printed regions seem a promising option. Once adjusted, following the methods proposed in this study, the manufacturing procedure can easily be turned into a pilot production line. However, some limitations and current research challenges, as well as future directions, are detected and foreseen, as detailed in the following section.

4 Current challenges and future research proposals

4.1 Limitations of the study and current research challenges

Regarding the 3D printing–assisted electroplating, it is important to take into account the limited dimensional and geometrical tolerances of FFF systems in general, which usually lead to very direct to manufacture components and constitute highly accessible systems but cannot yet compete with other high-precision industrial manufacturing systems. Even within the realm of additive manufacturing, FFF has never been the geometrical gold standard, as technologies including VAT-photopolymerization and powder bed fusion usually lead to better results. Having said this, FFF

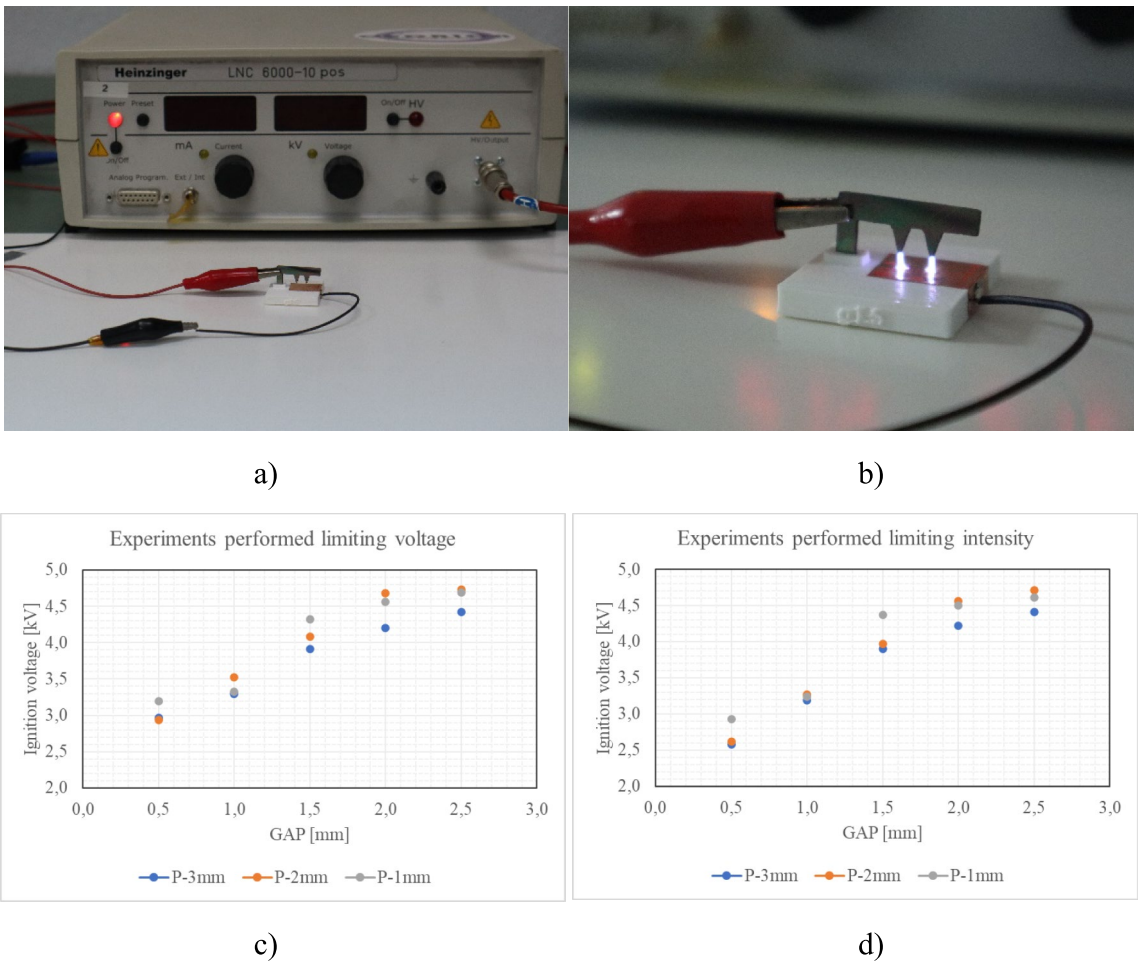

Fig. 7 The experimental setup for the streamer discharge (**a**) and the actual discharge after ignition (**b**). Images of the experiments and the summarizing graphs derived from Table 3 are shown in both for tests performed with limiting voltage (**c**) and with limiting intensity (**d**). Additional insights can be obtained in the supplementary materials including videos of the streamer discharge (S1 & S2)

is remarkable for its friendly usability and has proven an almost perfect companion to electroplating in this research. Nevertheless, some manufacturing limitations perceived in this technological combination have been detected as research challenges.

By means of example, Fig. 8 illustrates the more remarkable defects that our team has found during the processing of the different samples. Although these defects affect less than 12% of the samples, corresponding to ca. 1 electrode with defect per wafer, it is important to understand their eventual appearance and to minimize them by knowing their causes. Among others, it is important to mention: presence of unexpectedly printed fibers due to printing movements without retraction (Fig. 8a), overgrowth in certain sharp regions (Fig. 8b), regions deviated from the desired shape (Fig. 8c) and detachment of printed masks during electroplating leading to the exposure of unwanted regions (Fig. 8d).

Compared to machining and micromachining, electroplating of nickel structures within 3D-printed boundaries allows for the generation of thin-walled structures and needle-like geometries, hence avoiding the challenging machining of nickel and preventing potential failures, especially when thicknesses of less than 1 mm are involved. Still, as regards achievable geometrical complexity, the generated structures have a certain degree of intricacy but can be considered quasi-2D or 2D ½. Towards the creation of more complex geometries in connection with mechanical metamaterials, other additive manufacturing approaches may be required and investigated among possible future direction described in the following subsection.

Considering the streamer discharge electrodes, the generated structural electrodes based on a design including a set of discharge tips joined by a L-shaped plate prove more mechanically stable and robust than more classical solutions based on thin cross-section filaments, which under long operations tend to fail due to mechanical integrity and degradation issues [32]. It is expected that these innovative structural electrodes, obtained by electroplating of nickel within

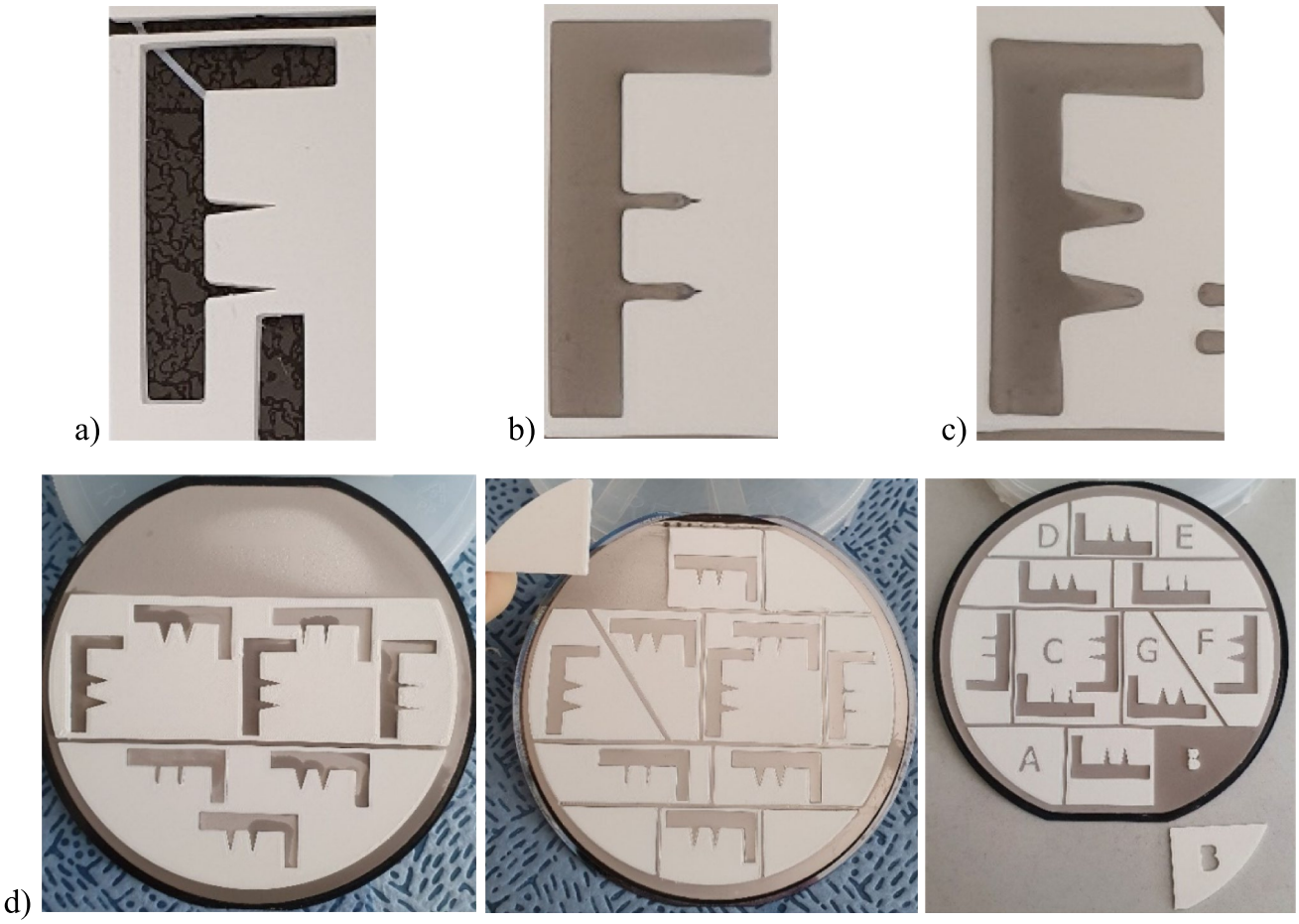

Fig. 8 Selection of possible manufacturing flaws found along the study in different experiments: **a** remaining printed fibers affecting the electroplating process, **b** overgrowth at thinner regions, **c** regions deviated from the desired shapes due to overgrowth, and **d** detachment of printed masks during electroplating leading to the exposure to nickel of unwanted regions

the printed contours, may degrade more progressively and prevent sudden failures, common in filament-based corona discharge generators, although this should be further studies.

4.2 Future directions

The currently achievable geometries with the presented process are quasi-two-dimensional, as the metal is grown starting from a planar substrate, with a desired external shape or pattern, but with homogeneous thickness and overall 2D aspect. Authors envision improvements in design and manufacturing freedom, leading to more versatile 3D geometries, by the employment of non-planar printing procedures upon curved substrates, for defining the electroplatable regions. Non-planar printing processes, also known as curved layer deposition procedures, have been explored for more than one decade [35–39] and seem to be getting more and more popular thanks to recent developments [40, 41]. The combination of these non-planar printing paths with other robotic-assisted fused deposition modelling or patterning processes [42, 43] could arguably lead to different levels of detail in the deposited protecting materials and, hence, promote the growth of non-planar metallic components and structures with hierarchical geometries. The use of multi-material extrusion nozzles employing different polymers reactive to diverse solvents could allow for multi-metallic non-planar electrochemical deposition, which would further increase the versatility of the process.

As regards dimensional and geometric tolerances, fused deposition modelling is still limited when compared to other additive manufacturing technologies based on high-precision lithographic and photopolymerization procedures, which on the other hand are often limited in terms of achievable part sizes and availability for their higher costs. Nevertheless, it would be interesting to explore the electroforming within multi-scale patterns achieved by combinations of UV-lithography, (micro-)laser stereolithography and multi-photon or two-photon absorption, and thus reach truly micro and nanomanufacturing details, following examples from

3D-printed masks applied to surface micromachining by etching [44, 45].

Considering the proposed industrial application to streamer discharge electrodes, next steps would focus on achieving more complex and larger electrodes capable of generating several discharges against a collecting electrode. To this end, inspiration in fractal geometries or models derived from applying the constructal law could prove aesthetically sounded, effective and efficient (https://web.archive.org/web/20181013014747/https://us.macmillan.com/books/9780716711865, http://www.fractal.org/topopleidingen/Fractalisme/Constructal-law.pdf). Surface functionalization and material transfer processes, based on the precise control of the generated micro-discharges and their localization (https://www.db-thueringen.de/servlets/MCRFileNodeServlet/dbt_derivate_00055792/ilm1-2022000023.pdf), possibly leading to a new micro-additive manufacturing strategy, should be researched as authors intend to do in the near future.

5 Conclusions

An innovative manufacturing method for selective electrochemical metal deposition has been developed and demonstrated, both with proof-of-concept geometries and through an industrial application. As described along the study, the proposed production chain hybridizes 3D printing and electroplating for the design-controlled electroforming of metals within fused deposition modelled contours or patterns, which provide a selective or guiding functionalization of the substrate for metal deposition on demand. Applying the developed process, Ni electrodes for streamer discharge plasma generators have been structured and experimentally evaluated. These components stand out for their needle-like details, required for promoting micro-lightnings, which would be challenging to obtain employing traditional milling processes. Current capabilities, main challenges and foreseen research directions, for this novel hybrid 3D printing and electroplating process and for its industrial applications, have been discussed. In the authors' opinion, the described process contributes to the already fruitful connections among additive manufacturing technologies and metal electrodeposition procedures, providing an interesting route towards accessible and straightforward electroforming of large-sized components and structures with fine details.

Supplementary Information The online version contains supplementary material available at https://doi.org/10.1007/s00170-025-15089-7.

Acknowledgements The support of the Karlsruhe Nano Micro Facility (KNMFi / https://www.knmf.kit.edu/), which supported the manufacturing of samples, is acknowledged. Karlsruhe Institute of Technology colleagues Dr. Uwe Köhler from the Institute of Microstructure Technology and Matthias Kuntzler from the Institute for Automation and Applied Informatics are acknowledged for their help with manufacturing processes.

Author contribution Mar Cogollo de Cádiz, Andrés Díaz Lantada, Tobias Müller and Markus Guttmann conceived the study and planned the research; Mar Cogollo and Andrés Díaz Lantada designed the innovative electrodes; Tobias Müller and Steffen Scholz developed and optimized the fused filament fabrication upon wafers; Markus Guttmann and Marco Ehrhardt developed and optimized the electroplating procedure and related postprocesses; Andrés Díaz Lantada and Sonia Ruíz Trujillo validated experimentally the industrial application; all authors contributed to writing and reviewing the paper and to scientific technological discussions.

Funding Open Access funding provided thanks to the CRUE-CSIC agreement with Springer Nature. S.R.T. and M.C.C. acknowledge the support of the "Programa de Doctorados Industriales" funded by the "Comunidad Autónoma de Madrid" (references: IND2020/17525 and IND2017/IND-7799, respectively) and of Cedrión C.T.I. S.L. A.D.L. acknowledges the support of the Karlsruhe Institute of Technology and its International Excellence Fellowship program that funded a research stay at KIT in 2023.

Data availability All relevant data for the paper are included in the manuscript. The authors will share the raw data from manufacturing trials and characterization tests on reasonable request, as well as the CAD models and blueprints from the different geometries designed.

Declarations

Conflict of interest The authors declare no competing interests.

References

1. Blum W, Hogaboom GB (1924) Principles of electroplating and electroforming (electrotyping) / by William Blum,... and George B. Hogaboom,... (McGraw-Hill book company, inc.)
2. (1924) Principles of electroplating and electroforming (electrotyping). Nature 114:272–272
3. McGeough JA (2014) Electroforming. In: Laperrière L, Reinhart G (eds) CIRP Encyclopedia of Production Engineering. Springer, pp 443–446. https://doi.org/10.1007/978-3-642-20617-7_6479
4. Madou MJ (2018) Fundamentals of Microfabrication and Nanotechnology, Three-Volume Set. CRC Press. https://doi.org/10.1201/9781315274164
5. Gad-el-Hak M (2001) The MEMS Handbook. CRC Press Inc, United States

6. Becker EW et al (1982) Production of separation-nozzle systems for uranium enrichment by a combination of X-ray lithography and galvanoplastics. Naturwissenschaften 69:520–523
7. Bley P, Bacher W, Menz W, Mohr J (1991) Description of microstructures in LIGA-technology. Microelectron Eng 13:509–512
8. Meyer P, Schulz J, Saile V (2010) Chapter 13 - Deep X-ray lithography. In: Qin Y (ed) Micro-Manufacturing Engineering and Technology. 202–220 William Andrew Publishing. https://doi.org/10.1016/B978-0-8155-1545-6.00013-2
9. Schelb M, Vannahme C, Kolew A, Mappes T (2011) Hot embossing of photonic crystal polymer structures with a high aspect ratio. J Micromech Microeng 21:025017
10. Ebraert E et al (2016) Hot-embossing replication of self-centering optical fiber alignment structures prototyped by deep proton writing. OE 55:076112
11. Müller T et al (2010) Ceramic micro parts produced by micro injection molding: latest developments. Microsyst Technol 16:1419–1423
12. Piotter V, Hanemann T, Ruprecht R, Haußelt J (1997) Injection molding and related techniques for fabrication of microstructures. Microsyst Technol 3:129–133
13. Wu W et al (2021) Snake-inspired, nano-stepped surface with tunable frictional anisotropy made from a shape-memory polymer for unidirectional transport of microparticles. Adv Func Mater 31:2009611
14. Xi W, Qiao Z, Zhu C, Jia A, Li M (2009) The preparation of lotus-like super-hydrophobic copper surfaces by electroplating. Appl Surf Sci 255:4836–4839
15. Huang H-X, Wang X (2019) Biomimetic fabrication of micro-/nanostructure on polypropylene surfaces with high dynamic superhydrophobic stability. Mater Today Commun 19:487–494
16 DíazLantada A et al (2015) Toward mass production of microtextured microdevices: linking rapid prototyping with microinjection molding. Int J Adv Manuf Technol 76:1011–1020
17. DíazLantada A et al (2018) Research on the methods for the mass production of multi-scale organs-on-chips. Polymers 10:1238
18 DíazLantada A et al (2020) Synergies between surface microstructuring and molecular nanopatterning for controlling cell populations on polymeric biointerfaces. Polymers (Basel) 12:655
19 DíazLantada A et al (2020) Soft-lithography of polyacrylamide hydrogels using microstructured templates: towards controlled cell populations on biointerfaces. Materials (Basel) 13:1586
20. Li X, Ming P, Ao S, Wang W (2022) Review of additive electrochemical micro-manufacturing technology. Int J Mach Tools Manuf 173:103848
21. Reiser A (2019) Additive manufacturing of metals at small length scales – microstructure, properties and novel multi-metal electrochemical concepts. ETH Zurich. https://doi.org/10.3929/ethz-b-000409601
22. Xia X et al (2019) Electrochemically reconfigurable architected materials. Nature 573:205–213
23. Liang Y et al (2023) Extruded 3D printing assisted electrochemical additive manufacturing. J Phys: Conf Ser 2463:012030
24. Mostafaei A et al (2023) Additive manufacturing of nickel-based superalloys: a state-of-the-art review on process-structure-defect-property relationship. Prog Mater Sci 136:101108
25. Vyatskikh A et al (2018) Additive manufacturing of 3D nano-architected metals. Nat Commun 9:593
26. Hassel T, Carstensen T (2020) Properties and anisotropy behaviour of a nickel base alloy material produced by robot-based wire and arc additive manufacturing. Weld World 64:1921–1931
27. Li R et al (2024) Simulation of residual stress and distortion evolution in dual-robot collaborative wire-arc additive manufactured Al-Cu alloys. Virtual Phys Prototyp 19:e2409390
28. Nijdam S, Teunissen J, Ebert U (2020) The physics of streamer discharge phenomena. Plasma Sources Sci Technol 29:103001
29. Syssoev VS et al (2022) Streamer discharge plasma generator. Inorg Mater Appl Res 13:1380–1384
30 Cogollo M, Balsalobre PM, DíazLantada A, Puago H (2020) Design and experimental evaluation of innovative wire-to-plane fins' configuration for atmosphere corona-discharge cooling devices. Appl Sci 10:1010
31 Cogollo de Cádiz M, MartíBalsalobre P, DíazLantada A (2022) Research on wire-to-two fin configuration for positive atmospheric plasma by electrokinetic blower. Energies 15:5443
32 Cogollo de Cádiz M, LópezArrabal A, DíazLantada A, Aguirre MV (2021) Materials degradation in non-thermal plasma generators by corona discharge. Sci Rep 11:24175
33. Deshpande YV, Andhare AB, Padole PM (2018) How cryogenic techniques help in machining of nickel alloys? A review. Mach Sci Technol 22:543–584
34. Jangali Satish G, Gaitonde VN, Kulkarni VN (2021) Traditional and non-traditional machining of nickel-based superalloys: a brief review. Mater Today: Proc 44:1448–1454
35. Chakraborty D, Aneesh Reddy B, Roy Choudhury A (2008) Extruder path generation for curved layer fused deposition modeling. Comp Aided Des 40:235–243
36. Diegel O, Singamneni S, Huang B, Gibson I (2011) Curve layer fused deposition modeling in conductive polymer additive manufacturing. Adv Mater Res 199–200:1984–1987
37. Singamneni S, Roy Choudhury A, Diegel O, Huang B (2012) Modeling and evaluation of curved layer fused deposition modeling. J Mater Process Technol 212:27–35
38. Chen L, Chung M-F, Tian Y, Joneja A, Tang K (2019) Variable-depth curved layer fused deposition modeling of thin-shells. Robot Comp Integr Manuf 57:422–434
39. Huang B, Singamneni S (2014) Curve layer fused deposition modeling with varying raster orientations. Appl Mech Mater 446–447:263–269
40. Ahlers D (2018) 3D printing of nonplanar layers for smooth surface generation. Master's Thesis, Universität Hamburg, Hamburg, Germany
41. Ahlers D, Wasserfall F, Hendrich N, Zhang J (2019) 3D printing of nonplanar layers for smooth surface generation. In: Proceedings of the IEEE 15th International Conference on Automation Science and Engineering (CASE), Vancouver, BC, Canada, pp 1737–1743
42. Brooks BJ, Arif KM, Dirven S et al (2017) Robot-assisted 3D printing of biopolymer thin shells. Int J Adv Manuf Technol 89:957–968
43. JustinoNetto JM, Idogava HT, Frezzatto Santos LE et al (2021) Screw-assisted 3D printing with granulated materials: a systematic review. Int J Adv Manuf Technol 115:2711–2727
44. Kanamori Y, Sato J, Shimano T et al (2007) Polymer microstructure generated by laser stereo-lithography and its transfer to silicon substrate using reactive ion etching. Microsyst Technol 13:1411–1416
45. Liu X, Bai B, Chen Q, Sun H (2019) Etching-assisted femtosecond laser modification of hard materials. Opto-Electronic Adv 2(9):190021